Virchows Arch (1996) 429:255–273
© Springer-Verlag 1996

ORIGINAL ARTICLE

Isao Shirato · Hiltraud Hosser · Kenjiro Kimura
Tatsuo Sakai · Yasuhiko Tomino · Wilhelm Kriz

The development of focal segmental glomerulosclerosis in Masugi nephritis is based on progressive podocyte damage

Received: 8 May 1996 / Accepted: 23 July 1996

Abstract We analysed the sequence of structural changes leading to focal segmental glomerulosclerosis (FSGS) in chronic Masugi nephritis. The protocol resulted in an immediate onset of the disease and the development of segmental sclerosis in a considerable proportion of glomeruli within 28 days of serum injection. Throughout the study, the degree of structural damage was significantly correlated with protein excretion. Even 1 day after injection of the serum, the whole spectrum of early lesions was encountered involving all three cell types. Endothelial detachments, mesangiolysis and podocyte foot process effacement were most prominent. There was focal persistence of capillary microthrombosis but, generally, mesangial and endothelial injuries recovered. The development of podocyte lesions was different: on one hand recovery was seen leading to the re-establishment of an interdigitating foot process pattern, and on the other persistent podocyte detachments from peripheral capillaries allowed the attachment of parietal epithelial cells to "naked" portions of the glomerular basement membrane (GBM), and thus to the formation of a tuft adhesion to Bowman's capsule. Progressive podocyte degeneration at the flanks of an adhesion permitted expansion of the adhesion by encroachment of parietal cells onto the tuft along the denuded GBM. Inside an adhesion, capillaries and mesangial areas either collapse or become obstructed by hyalinosis or thrombosis. Resident cells disappear progressively from inside an adhesion; macrophages may invade. Segmental sclerosis in this model consists of collapsed tuft structures adhering broadly to the cortical interstitium. Proliferation of mesangial cells did not contribute to this development. Recovery of endothelial and mesangial lesions was associated with cell proliferation in early stages of the disease; podocyte proliferation was not encountered at any stage. We conclude that the inability to replace an outmatched podocyte crucially underlies the development of sclerosis. Severe podocyte damage cannot be repaired but leads to tuft adhesions to Bowman's capsule followed by progressive collapse of tuft structures inside an adhesion, resulting in segmental glomerulosclerosis.

Key words Masugi nephritis · Glomerular damage · Podocytes · Focal segmental glomerulosclerosis

I. Shirato · H. Hosser · W. Kriz (✉)
Institut für Anatomie und Zellbiologie,
Im Neuenheimer Feld 307, D-69120 Heidelberg, Germany
Tel.: (49) 62 21-54 86 80, Fax: (49) 62 21-54 49 51

K. Kimura
Second Department of Internal Medicine,
Tokyo University, Tokyo, Japan

T. Sakai
First Department of Anatomy, Juntendo University, Tokyo, Japan

I. Shirato · Y. Tomino
Division of Nephrology, Department of Medicine,
Juntendo University, Tokyo, Japan

Introduction

Masugi nephritis is the classic model for experimental glomerulonephritis. Injection of heterologous anti-kidney sera into rats and rabbits leads to a progressive kidney disease, eventually terminating in chronic renal failure resembling human glomerulonephritis in many respects [9].

Considerable progress has been achieved in the understanding of the pathogenic mechanisms since the first description [27]. The initial heterologous phase of Masugi nephritis is mediated by heterologous antibodies binding to the glomerular basement membrane (GBM), followed by attraction of leucocytes to the glomeruli [5]. Subsequently, the production of autologous antibodies against the heterologous antibodies maintains the disease, which is associated with infiltration of monocytes/macrophages into the glomerulus [46]. Haemodynamic factors, especially the rise in glomerular capillary pressure, advance development of the disease [2, 26, 32, 33]. Recent studies have dealt with the relevance of cytokines and growth factors in the pathogenesis of this nephritis [18, 47], and it has been shown that antibodies against integrins contained in Masugi sera may have con-

siderable impact on the development of the disease, by disconnecting glomerular cells from the GBM [36].

Nonimmune factors appear to play the dominant role in the ultimate decline of renal function [10, 32, 33]. Histopathologically, this decline results from progressive nephron loss following a glomerular degeneration pattern known as focal segmental glomerulosclerosis [17]. It is widely assumed that mesangial proliferation and mesangial matrix deposition are the major pathologic mechanisms underlying the progression to sclerosis. In the light of more recent findings in several other models of FSGS, in which failure of podocytes was shown to be the decisive step for sclerosis development [19, 21, 30], the present study has reevaluated the step-by-step sequence of structural changes in glomeruli terminating in segmental sclerosis in Masugi nephritis. Part of this study dealing exclusively with the process of foot process effacement of podocytes has been published elsewhere [44].

Materials and methods

Male Sprague-Dawley rats (weighing 150–170 g) were obtained from Charles River Japan (Kanagawa, Japan). Animals were kept in an air-conditioned room and maintained on a commercial stock diet and tap water ad libitum.

Masugi nephritis was induced by single intravenous injection of rabbit anti-rat GBM serum (0.1 ml/100 g body weight). Rabbit anti-rat GBM serum was kindly provided by Yoshio Suzuki and Tadashi Nagamatsu (Faculty of Pharmacology, Meijo University, Nagoya, Japan). In addition to a control group (no injection) six experimental groups with animals sacrificed 4 h, and 1, 3, 7, 10, and 28 days after the injection were studied. Each group (except the 4 h and 7 day groups) consisted of six rats; four in each group were used for structural studies and two for immunocytochemistry. The 4 h and 7 day groups each consisted of only two rats, which were used for structural studies. One day before sacrifice, all rats (except the 4 h and 7 day groups) had a 24-h urine collection to determine total protein excretion. Urinary protein concentration was determined by using Tonein TP kit (Coomasie brilliant blue G250: Otsuka Pharmacy, Tokyo, Japan).

At the time of death, the kidneys were fixed by total-body perfusion as described previously [16]. Briefly, after anaesthesia with Nembutal (100 mg/kg body weight) the abdominal cavity was opened and the kidneys were retrogradely perfused via the abdominal aorta without prior flushing of the vasculature. Perfusion pressure in the perfusion apparatus was 200 mmHg; perfusion was maintained for 3 min.

For structural studies the fixative contained 2% glutaraldehyde in 0.1 M sodium phosphate buffer (PBS) at pH 7.4. After perfusion, the kidneys were removed and immersed in the same fixative overnight. Tissue was then processed in a modified postfixation and staining technique that minimizes treatment with osmium tetroxide and uses tannic acid as a contrast agent (including dehydration in cold acetone) [39, 43]. All tissues were finally embedded in Epon 812 by standard procedures. Semithin sections (1 μm) stained with toluidine-blue were used for light microscopy (Polyvar 2, Reichert-Jung, Vienna, Austria) and morphometry. Ultrathin sections stained in uranyl acetate and lead citrate were observed in a Philips EM 301 (Philips Electronics, Eindhoven, The Netherlands).

For immunocytochemistry, the kidneys were fixed by perfusion (see above) with a fixative containing 2% paraformaldehyde in 0.1 M PBS (pH 7.4). They were removed, and pieces of the right kidney were immediately snap-frozen in melting isopentane and stored in liquid nitrogen. Frozen sections 5 μm thick were cut on a Reichert 2800 Frigocut (Reichert-Jung, Vienna, Austria) and fixed with ice-cold acetone. Immunostaining of the sections was done with the indirect immunofluorescence technique by using a monoclonal mouse anti-desmin antibody (Clone DE-U-10, Sigma, St. Louis, Mo.) as a first antibody and a FITC-conjugated goat anti-mouse IgG (Cappel, Denkendorf, Germany) as a second antibody. The antibody against desmin was diluted 1:20 in PBS containing 1% BSA. After immunostaining, the sections were examined by epifluorescence in a Reichert Polyvar microscope and photographed using Kodak Tri-X PAN film.

Morphometric analysis was carried out with a semiautomatic image analysis system (VIDS IV, Ai Tectron, Düsseldorf, Germany). Mean glomerular tuft volume (VT) was determined according to Weibel [49]. For each animal, 60 consecutively encountered glomeruli were analysed. Surface areas of the glomerular tufts (AT) were determined in 1-μm sections under direct visualization (magnification×690) in a blind fashion. VT was calculated according to the formula $VT = (\beta/k)(A)^{3/2}$, where $\beta = 1.38$ (a shape coefficient), $k = 1.1$ (size distribution coefficient for spheres), and A = mean AT.

The degree of foot process fusion was estimated as the fraction of outer capillary surface covered with non-interdigitating podocyte portions. The point counting method was applied [49]. A multipurpose test system was overlaid on light micrographs (final magnification×1280) of four glomerular profiles per animal, randomly sampled in epon-embedded 1-μm sections. Intersections of test lines with a capillary wall covered at the site of intersection either by foot processes or by noninterdigitating podocyte portions were evaluated. In each animal roughly 200 intersection points were considered.

To estimate the degree of glomerular damage, glomerular lesions were scored as follows. In 1-μm sections 60 consecutively encountered glomeruli per animal were screened under the light microscope in a blind fashion. Pseudocysts, tuft appositions, tuft adhesion to Bowman's capsule and segmental sclerosis were included in the evaluation in a graded weighing [44]. Glomeruli with pseudocysts only were factored by 1, glomeruli with appositions, by 2 (generally containing pseudocysts), and glomeruli with adhesions or segmental sclerosis, by 3. The sum of these values in each animal was considered to reflect the degree of damage. A tuft adhesion to Bowman's capsule was classified as segmental sclerosis when the adherent tuft area contained collapsed, hyalinized or otherwise obstructed capillaries.

Results are reported as mean ± standard deviation (SD). Group differences were assessed by one-way ANOVA followed by Scheffe multiple range test. Correlation analysis between glomerular damage (damage index), tuft volume, and urinary protein excretion was done by Spearman's rank correlation test. All statistical calculations were performed with the SPSS analysis program (Chicago, Ill.).

Results

As has been shown previously [23, 42], glomerulonephritis developed quickly after serum application, which was reflected in a rapid rise in urinary protein excretion (Table 1). Throughout the study, protein excretion was significantly correlated with the degree of structural damage. Up to day 10, a good correlation was also seen between damage score and protein excretion on the one hand and tuft growth/hypertrophy on the other ($rs = 0.669$; $P<0.02$ and $rs = 0.786$; $P<0.01$, respectively). Thereafter, tuft volume increased further, together with a significant increase in the incidence of sclerosis, whereas the overall damage score (which also takes account of presclerotic lesions) and a proteinuria decreased slightly (Table 1). The number of podocytes per glomer-

Table 1 Urine and glomerular data. [U Prot, urinary protein excretion; V Bow, renal corpuscle volume (volume enclosed by Bowman's capsule); V Tuft, glomerular tuft volume; V Tuft/V Bow, ratio between tuft and corpuscle volume; N Pod/Glom, number of podocytes per glomerular profile; D Pod/A Tuft, numerical density of podocytes per glomerular tuft area; N Pod binucl/Glom, number of bi(multi)nucleated podocytes per glomerular profile;% Glom with sclerosis, percentage of glomerular profiles with segmental sclerosis;% Glom with adhesion, percentage of glomerular profiles with tuft adhesions to Bowman's capsule; damage index, glomerular damage index as defined in Material and methods;% area without foot process pattern, percentage of outer capillary area not covered with interdigitating foot processes (correlates with the degree of foot process effacement)

	U Prot (mg/day)[a]	V Bow ($m^3 \times 10^6$)	V Tuft ($m^3 \times 10^6$)	V Tuft/ V Bow ($m^3 \times 10^6$)	N Pod/ Glom	D Pod/ A Tuft ($N/m^2 \times 10^4$)	N Pod binucl/ Glom	% Glom with sclerosis[a]	% Glom with adhesion	Damage index[a]	% Area without foot process pattern[a]
Day 0 (control)	11.7	1.63	1.07	0.63	10.2	11.7	0.09			0.5	18
(n=4) SD	2.4	0.38	0.32	0.06	1.5	3.0	0.07			1	3.8
Day 1 (control)	290.6	1.70	1.27	0.71	10.5	10.5	0.26		0.4	28.5	87
(n=4) SD	60.3	0.21	0.15	0.04	1.6	2.2	0.14		0.9	2.7	6.8
Day 3 (control)	386.1	2.08	1.65	0.77	9.7	8.1	0.59		0.9	96.8	92.5
(n=4) SD	26.7	0.11	0.09	0.04	1.3	1.4	0.14		1.0	5.1	1.7
Day 10 (control)	486.8	2.91	2.04	0.68	9.3	6.7	1.20	3.7	26.5	111.5	83
(n=4) SD	112.6	0.34	0.16	0.06	1.6	1.1	0.23	3.2	11.4	17.1	13.9
Day 28 (control)	359.5	3.85	2.65	0.67	8.3	5.1	0.64	28.8	32.8	97.5	53.3
(n=4) SD	65.4	0.36	0.28	0.01	1.0	0.6	0.53	16.5	16.1	21.4	3.5
P<0.01	c vs d1 c vs d3 c vs d10 c vs d28	c vs d10 c vs d28 d1 vs d10 d1 vs d28 d3 vs d28 d10 vs d28	c vs d10 c vs d28 d1 vs d10 d1 vs d28 d3 vs d28	c vs d3		c vs d28 d1 vs d28	c vs d10 d1 vs d10	c vs d28 d1 vs d28 d3 vs d28 d10 vs d28	c vs d28 d1 vs d28 d3 vs d28	c vs d3 c vs d10 c vs d28 d1 vs d3 d1 vs d10 d10 vs d28	c vs d1 c vs d3 c vs d10 c vs d28 d1 vs d28 d3 vs d28

[a] Values in these columns have already been published [17]

ular profile did not change significantly throughout the study (though there was a clear tendency to decrease) but – based on glomerular growth – podocyte density decreased dramatically, so that by day 28 it was less than the half the control value on day 0.

In agreement with previous studies [23, 42] severe structural damage was seen comprising the entire population of glomeruli. For descriptive purposes it seems appropriate to distinguish early lesions (up to day 3, thus belonging to the heterologous phase [23]), intermediate lesions (comprising observations from day 7 and 10 of the disease, thus belonging to the autologous phase [23]) and late lesions (day 28), which already included a high proportion of segmental glomerulosclerosis. Thus, the material abundantly contained the whole sequence of lesions terminating in glomerulosclerosis. The term "glomerulosclerosis" is used in the definition given by Rennke [37] as the glomerular lesion that "consists of global or segmental collapse of capillaries with disappearance of the cellular elements and microvascular lumina, entrapment of foamy macrophages, cellular debris and hyaline material, also known as hyalinosis and adhesion of the tuft to Bowman's capsule by synechia."

Early lesions

As seen in previous studies [17, 23, 42] extensive mesangial and endothelial changes from 4 h after serum administration were encountered. Widespread mesangiolysis apparently resulted from mesangial cell death, mesangial cells had frequently disappeared from expanded mesangial areas. Detachments of the endothelium from the GBM allowed expansion of the mesangium into subendothelial spaces; endothelial defects resulted in the adhesion of blood cells (neutrophils and macrophages) to denuded inner capillary surfaces.

Podocyte lesions developed somewhat later; they were not seen 4 h after serum administration, but after 1 day podocytes were fairly uniformly affected. The most prominent lesion was foot process effacement, leading to a dramatic disappearance of an interdigitating foot process pattern: at day 3 only 8% of outer capillary surfaces were still decorated with foot processes (Table 1). A detailed structural analysis of changes associated with foot process effacement has been published elsewhere [44]. In addition, pseudocyst formation and microvillous transformation were seen. In the most severe cases, detachment of podocytes from the GBM was encountered as early as at day 1.

These initial lesions affecting the endothelium, the mesangium and the podocytes were associated with overall changes in tuft architecture, which were clearly seen on day 3 (Fig. 1). The tufts appeared to be blown up as a result of expansion of mesangial areas and of distorted and ballooned capillaries. The tuft as a whole, an entire lobule, or individual capillaries approached the parietal epithelium more closely than usual with podocyte cell bodies prolapsing into the proximal tubule orifice (Fig. 1).

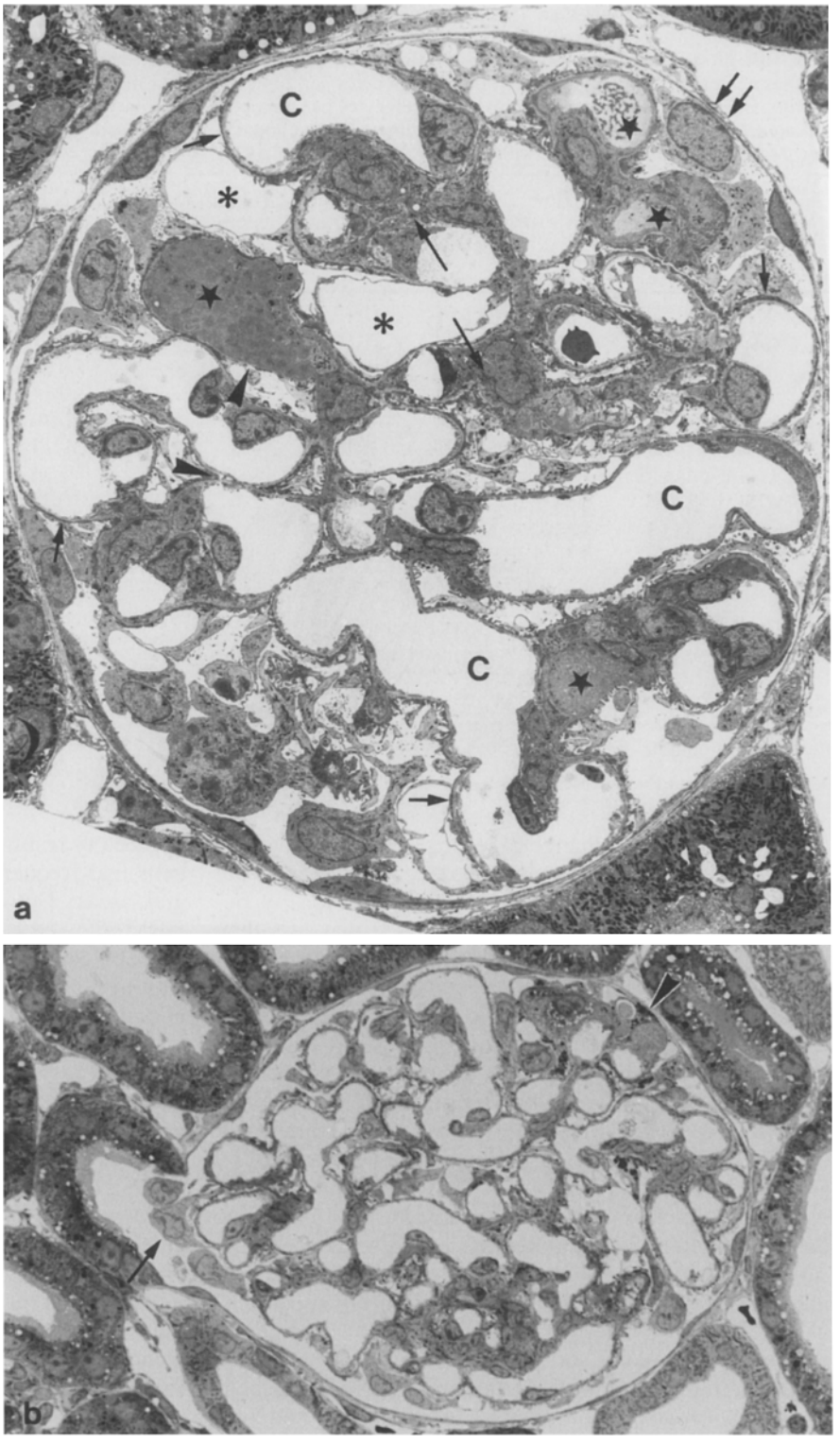

Fig. 1a, b Glomerular lesions resulting in tuft expansion. **a** Glomerular profile exhibiting a plethora of pathological changes. Podocytes show widespread foot process effacement (*small arrows*), pseudocyst formation (*asterisks*), microvillous transformation and discrete detachments from the glomerular basement membrane (GBM) (*arrowheads*). Several capillaries are occluded by fibrinoid or hyaline material (*stars*). Mesangiolysis is less obvious than in earlier stages; in its stead, mesangial proliferation is seen at some sites (*long arrows*). The tuft as a whole appears expanded; ballooned peripheral capillaries (*c*) and, consequently, podocytes come very close to the parietal epithelium or are even apposed to it (*two arrows*). **b** A further example of glomerular tuft expansion showing the prolapse of three podocytes into the orifice of the proximal tubule (*arrow*) and the apposition of a deteriorated tuft area to Bowman's capsule (*arrowhead*). **a** Masugi nephritis (MaNe) day 3, TEM, ×~1100; **b** MaNe day 28, LM, ×~525

Fig. 2a–c Damage pattern on day 10. **a** Overview. The situation is dominated by severe podocyte injury, including foot process effacement, pseudocyst formation (*asterisks*), accumulation of absorption droplets (*arrowheads*) and extensive detachments from the *GBM* (*arrows*). A dilated peripheral capillary loop (*C*) situated opposite to the vascular pole (*VP*) is attached to the basement membrane of the parietal epithelium establishing a circumscribed adhesion. Parietal cells adhere to the flanks of this adhesion. **b** An enlarged view of this area from a consecutive section, showing the attachment in more detail. Contact is established between the naked GBM surrounding the capillary loop (which at this site is obstructed) and the multilayered basement membrane of the parietal epithelium (*PBM*). Parietal cells adhere to the flanks of this capillary from both sides (*arrows*). At several sites cellular debris in Bowman's space is seen (*stars*). **c** One of those areas enlarged, suggesting that this debris results from dissolution of a podocyte. Endothelial defects are still encountered but are less prominent than in earlier stages of the disease. The mesangium is comparatively unremarkable ▶

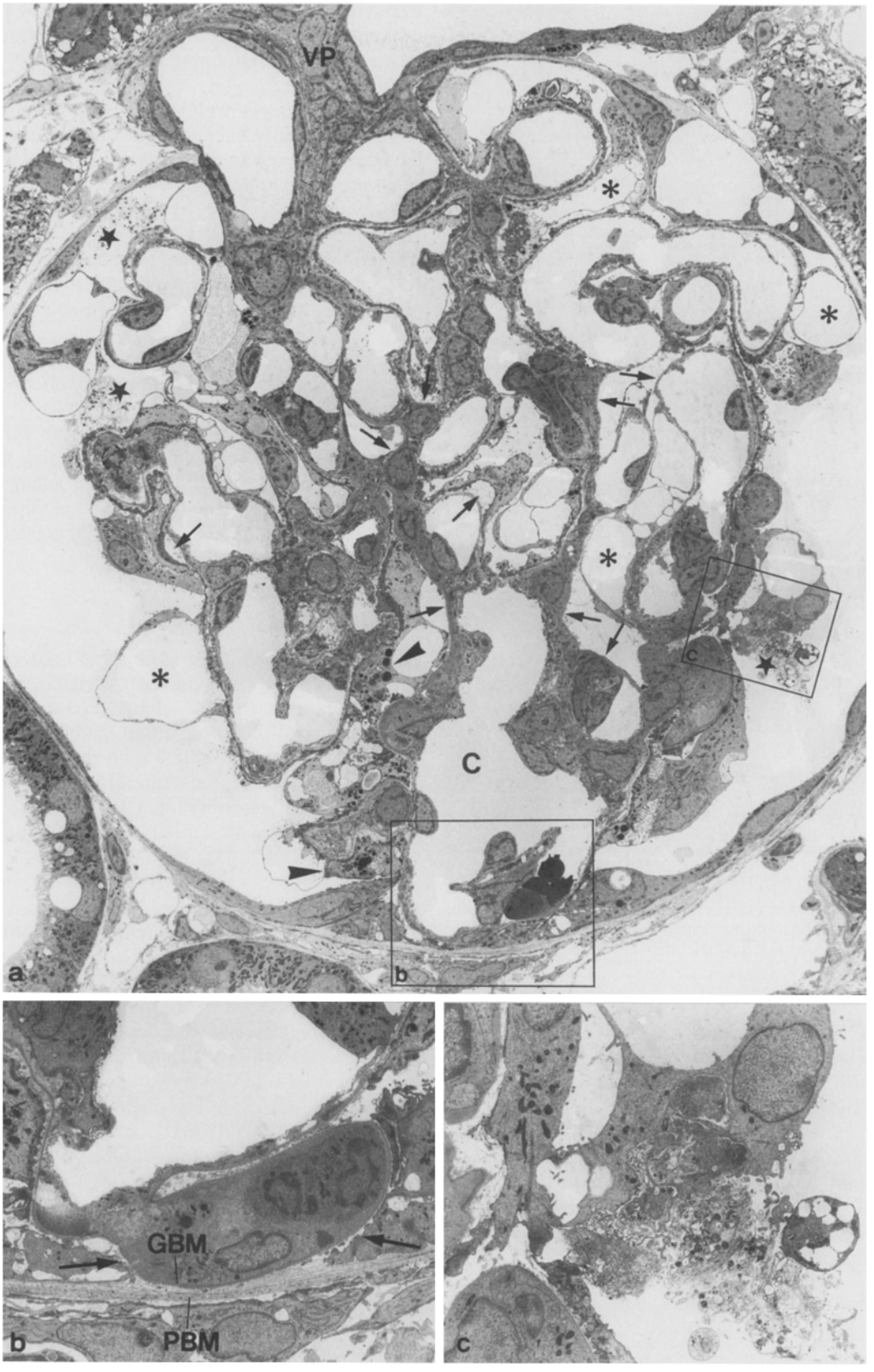
VP
C
a
b
c
GBM
PBM
b
c

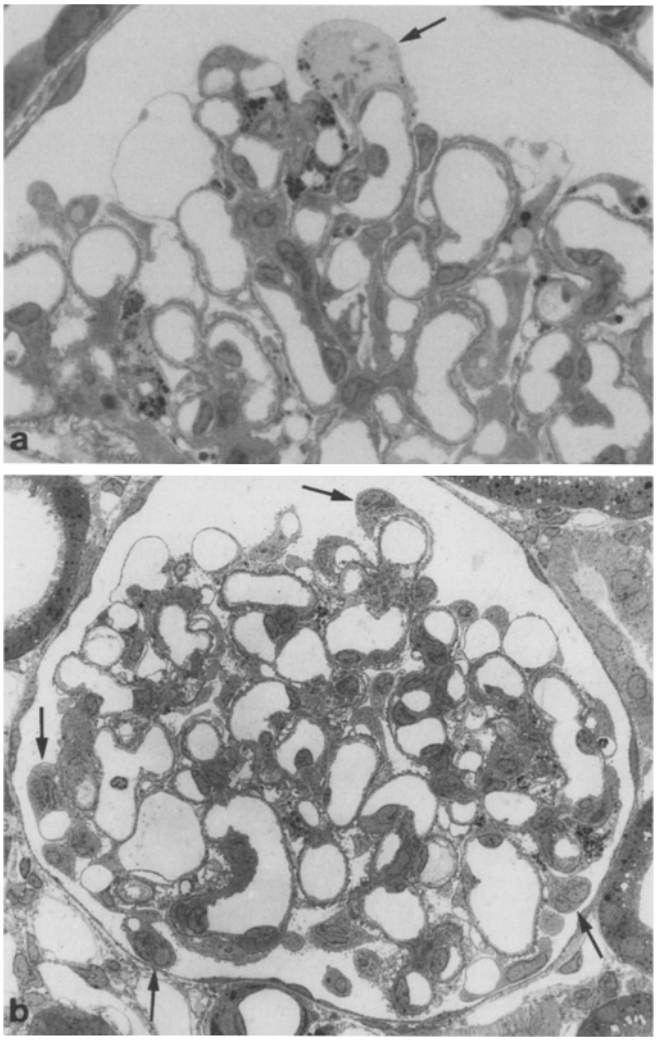

Fig. 3a, b Mitosis/binucleated podocytes. **a** A mitotic figure in a peripherally located podocyte is seen (*arrow*). **b** A glomerular profile in which several bi(multi)nucleated podocytes are seen, all located peripherally (*arrows*). **a** MaNe, day 7. LM, ×~700. **b** MaNe, day 7. TEM, ×~480

At day 3, in parallel with the persistence of widespread podocyte damage, recovery from endothelial and mesangial lesions was clearly seen. Most capillaries were patent and outlined by an intact endothelial covering. Focally, however, capillary profiles were occluded with microthrombi or with fibrinoid or hyaline material (Fig. 1). Mesangiolytic areas were replaced by mesangial tissues consisting of highly branched mesangial cells embedded into a dense extracellular matrix. Focally, mesangial hyalinosis was seen (Fig. 1).

Intermediate lesions

The pattern of glomerular lesions characteristic for an intermediate stage of damage development are all displayed in an overview of a single glomerular profile (Fig. 2). Most prominent were architectural changes; they consisted in widespread distortion of tuft structure including derangements of the folding pattern of capillaries as well as ballooning of capillaries.

No fresh mesangial lesions (mesangiolysis) and no endothelial defects were seen; endothelial detachments were occasionally encountered. In contrast, severe podocyte lesions were seen throughout the entire population of glomeruli. Compared with day 3, these lesions were more extensive and focally more advanced. Detachments of podocytes from the GBM, leaving behind extensive denuded GBM areas, were frequently encountered, corroborating the finding of apparently exhausted podocytes and podocyte cell debris in Bowman's space (Fig. 2). Bi(multi)nucleated podocytes were seen in comparably high numbers (Table 1, Fig. 3). Mitotic figures in podocytes (Fig. 3) were most frequently encountered in this stage of the disease.

The most severe lesions in this stage were tuft adhesions to Bowman's capsule (Fig. 2), which were encountered at high frequency (Table 1). In adherent tuft areas capillaries were often occluded and macrophages had invaded capillary lumina and mesangial areas (see below).

Late lesions

At day 28, damage progression and recovery were seen side by side (Fig. 4). On the one hand, glomerular lesions had advanced to sclerosis (comprising 32% of glomerular profiles on average, and more than 40% in two of the animals; Table 1), on the other, in the same kidneys and even in the same glomeruli just beside the sclerotic areas, recovery of a foot process pattern was seen. Compared with day 10, when little foot process interdigitation was left, at day 28 almost 50% of the outer capillary surface was redecorated by an interdigitating pattern (Table 1).

Damage progression was manifest in continual formation of tuft adhesions and their progression to segmental sclerosis (Figs. 5–9). By day 28, all stages of sclerosis development were seen. Large synechiae and small circumscribed adhesions were found side by side in neighbouring glomeruli of the same kidney. In some glomeruli the process of sclerosis had started in the early stages of the disease and those early adhesions had advanced to extensive synechiae. However, this process also appeared to start afresh with the formation of new "one-capillary-loop adhesions" at any time.

Segmental sclerosis was encountered throughout the tuft circumference, at the vascular pole, at the urinary pole as a so called "tip lesion" [15] and at all sites in between. Glomeruli with multiple synechiae were also frequently seen (Fig. 9).

Sequence of lesions leading to segmental sclerosis

Detachments of podocytes from the GBM were encountered at any stage of the disease from day 1 onward.

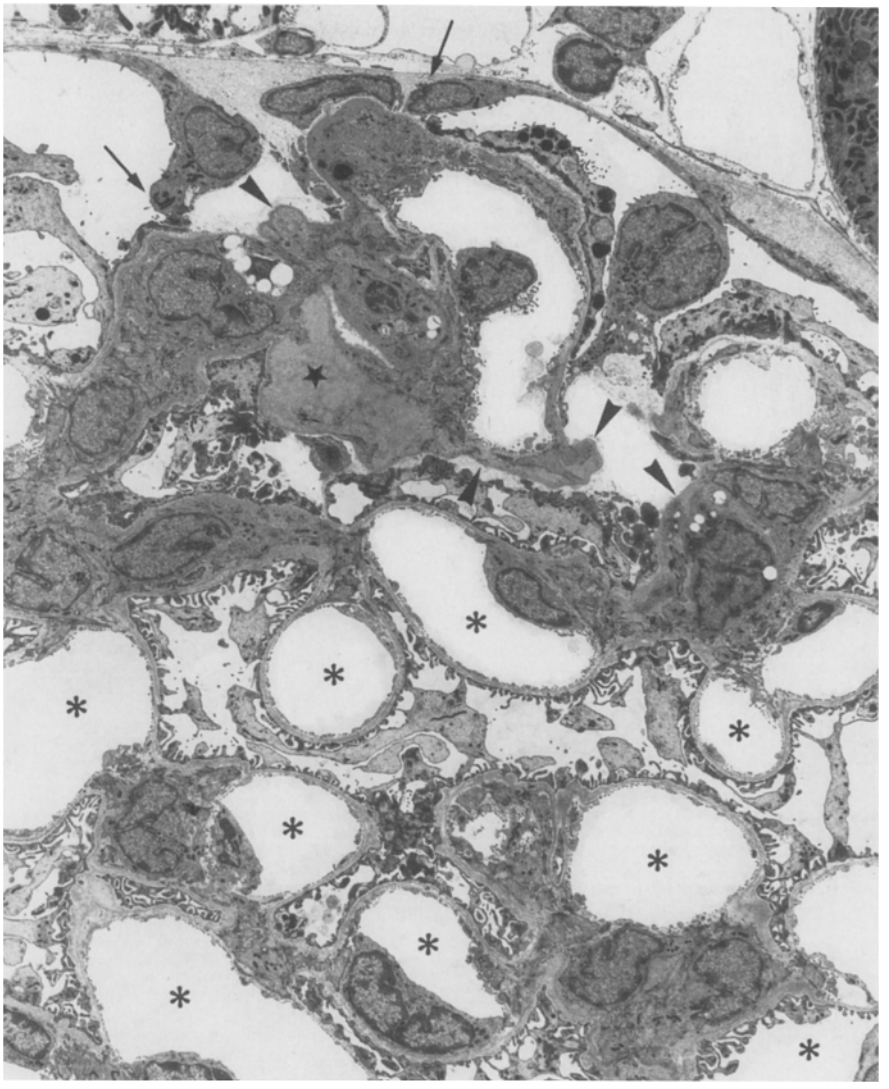

Fig. 4 Day 28 – overview. In late stages of the disease regenerating areas are seen side by side with areas showing progression to sclerosis. Capillaries in the *lower half* of the figure are patent (*asterisks*) and redecorated with an interdigitating foot process pattern. In contrast, in the *upper portion* podocyte foot process effacement, detachment of podocytes from the GBM (*arrowheads*), hyalinosis (*star*) and a tuft adhesion to Bowman's capsule are seen. Parietal cells typically adhere to both sides of the adhesion (*arrows*). MaNe, day 28. TEM, ×~2100

These increased in frequency in later stages and were seen in all areas of the tuft, central as well as peripheral. Two kinds of podocyte detachments were seen. Partial detachments consisted of a punctate pattern of disconnections between podocytes and the GBM; this pattern was generally associated with foot process effacement. As described in more detail elsewhere [44] this kind of detachment appeared to have a good chance of recovery. More complete detachments resulted in extensive areas of denuded GBM. In those areas podocytes frequently appeared to disconnect from the GBM in toto, or at least with a considerable proportion of their processes (Figs. 2, 4). Such widespread denudations of the GBM were generally associated with hyalinosis accumulating locally behind the GBM within capillaries and/or mesangial areas.

Denudation of peripheral capillaries in conjunction with a centrifugal expansion of those capillaries toward Bowman's capsule led to the apposition of naked GBM portions to the parietal epithelium (Fig. 5a). Such appositions are interpreted as the immediately preceding lesion and the sine qua non for the formation of a tuft adhesion to Bowman's capsule. Tuft adhesions consistently exhibited parietal cells affixed to naked GBM areas.

For descriptive purposes tuft adhesions can be classified as small, intermediate and large; the latter represent synechiae and, thus, fully developed segmental sclerosis. Small circumscribed adhesions generally displayed the sort of organization (seen in Figs. 2 and 5b). One or two capillary loops were involved; in a substantial proportion of cases these capillaries were occluded. Two neighbouring parietal cells were attached to the flanks of the adhesion, leaving a gap between the two attachment sides, where the "naked" GBM directly faced the parietal basement membrane of Bowman's capsule. The podocytes decorating the flanks of such an adhesion commonly exhibited severe lesions, including foot process effacement, pseudocyst formation, cytoplasmic accumulation of absorption droplets and detachments from the GBM.

Such small adhesions were found at any site of the tuft circumference, including positions opposite to the vascular pole. Glomerular profiles with up to three indi-

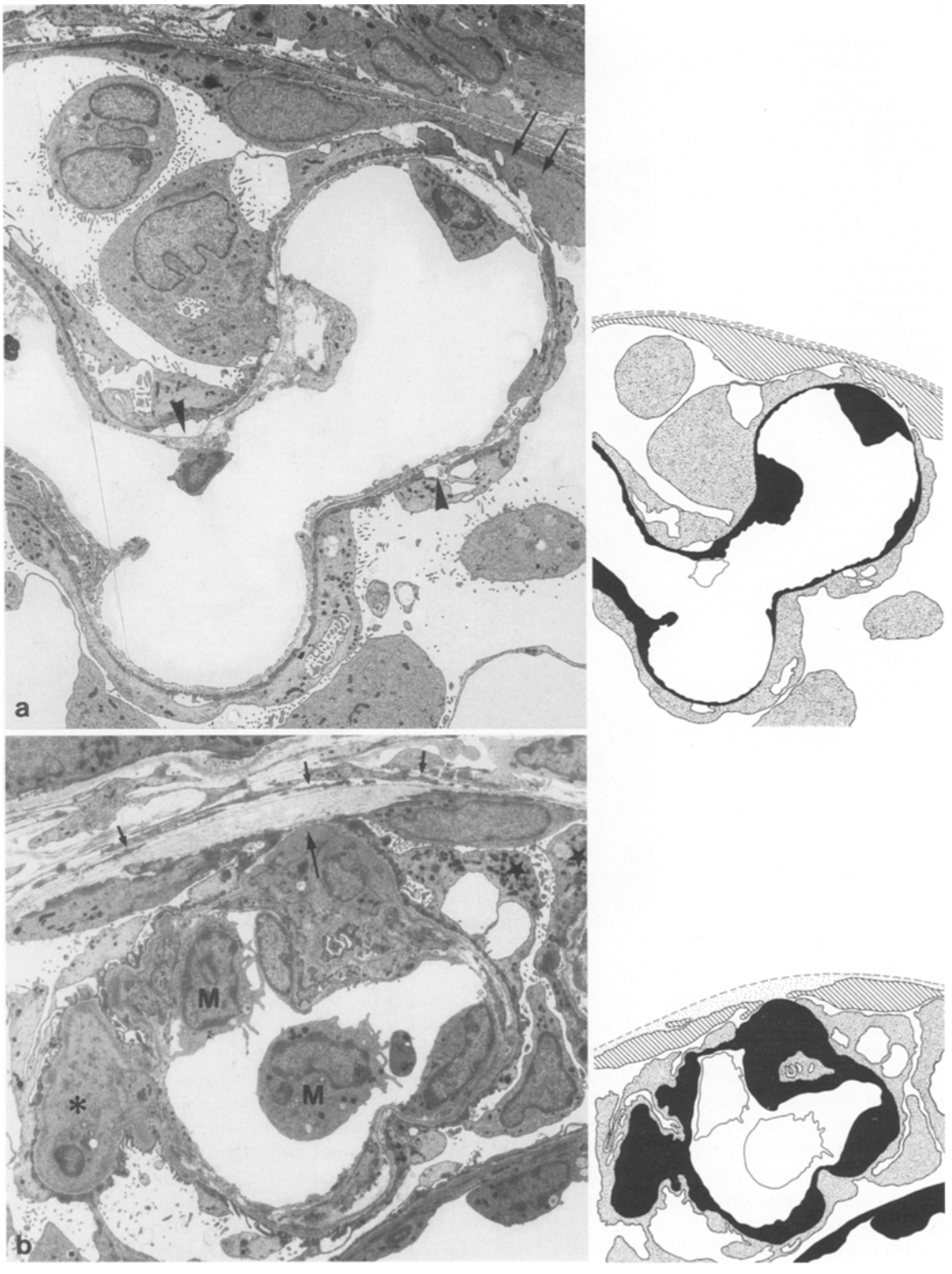

Fig. 5a, b Apposition and early tuft adhesion. **a** Apposition of a denuded capillary area to the parietal epithelium (*arrows*). Beneath this area the endothelium is also disconnected from the basement membrane. Partial detachments of podocytes from the GBM are also seen at other sites (*arrowheads*). Note widespread foot process effacement. **b** Adhesion of a capillary loop to Bowman's capsule. The parietal epithelium attaches from both sides to the flanks of the adhesion. In between these attachment points a gap in the parietal epithelium has come into existence; at this site (*arrow*) a denuded area of the GBM is in direct contact with the expanded parietal basement membrane of Bowman's capsule (cf. the normal multilayered appearance of this basement membrane as seen in **a**). Beneath this attachment site hyalinosis is seen inside the GBM. Towards the cortical interstitium the parietal basement membrane is delineated by sheet-like processes of cortical fibroblasts (*small arrows*). Podocytes at the flanks of the adhesion (*stars*) show accumulation of absorption droplets and foot process effacement. Note the macrophages (*M*) in the capillary lumen; another segment of this capillary is occluded by hyaline material (*asterisk*). In the drawings the GBM, including all structures that adhere to the GBM from inside, is shown in *black*, podocytes are *densely stippled*, parietal cells are *hatched*. The multilayered structure of the parietal basement membrane is indicated by *hatched lines*; expanded areas of the parietal basement membrane with dissolution of lamina densa material are *stippled*. **a** MaNe day 3, TEM, ×~4700; **b** MaNe day 7, TEM, ×~2000

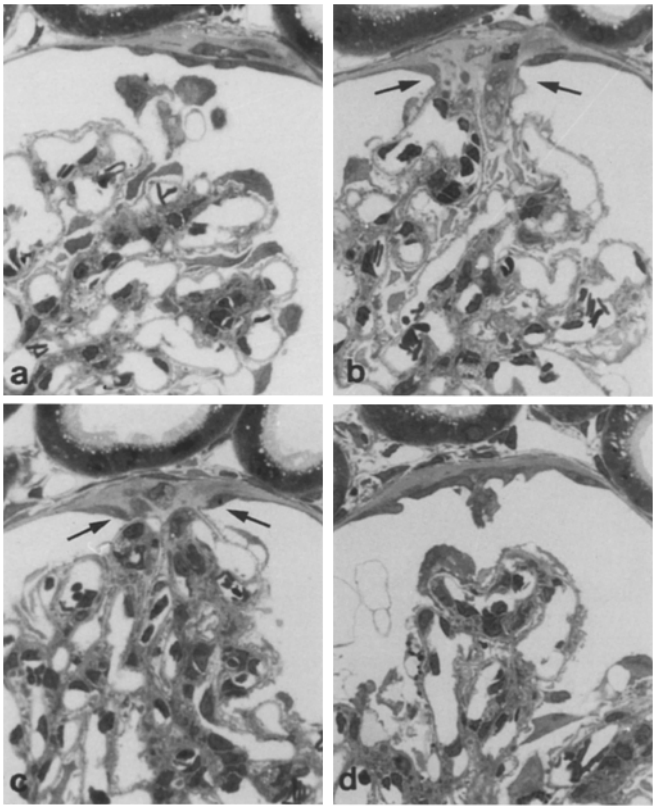

Fig. 6a–d Extension of a small tuft adhesion. Series of light micrographs to show the extension of an adhesion comprising two capillary loops. **a** Beginning of the adhesion, **b, c** sections through central parts of the adhesion, **d** the end. In **b** and **c** the attachment points of the parietal epithelium to the flanks of the adhesion (*arrows*) and the gap towards the cortical interstitium are clearly seen. MaNe day 28, LM series, ×~450

vidual circumscribed adhesions were also encountered. By tracing in serial sections at the light microscopic level it was confirmed that this kind of adhesions designated as "small" in individual electron micrographs really comprised a circumscribed tuft portion of one or few capillary loops (Fig. 6).

Adhesions of intermediate size, comprising three to several capillary loops, clearly appeared to have developed from small adhesions by incorporation of additional capillary loops (Fig. 7). Inside such an intermediate adhesion capillaries had collapsed (leaving behind wrinkled GBM profiles), were partially or totally occluded by microthrombosis, or were uniformly filled with hyaline material. Podocytes had generally disappeared from the interior of an adhesion. Most of the cells that have survived inside adhesions appear to be mesangial cells. Signs of mesangial cell proliferation, de novo matrix synthesis and deposition were not encountered.

Large adhesions typically represent what is called segmental sclerosis. The composition of such a synechia is no different from that of an adhesion of intermediate size, suggesting that a large adhesion has grown from an intermediate one by the encroachment of the sclerotic process onto an entire lobule. The glomerular profile shown in Fig. 8 exhibits the salient features of such synechiae. The appearance of such large adhesions was extremely multiform, but there was a basic pattern of individual lesions. Inside the GBM capillaries were either collapsed, hyalinized or otherwise occluded. Together with collapsed or hyalinized mesangial areas these tuft remnants make up what may be called "sclerotic formations". Inside those collapsed GBM formations, cells were sparse, and frequently completely absent. Macrophages were found in varying numbers exclusively located inside the GBM and thus within former capillary lumina or mesangial areas. Outside the GBM (but inside the adhesion) podocytes have disappeared. Podocytes situated at the flanks of an adhesion exhibited quite serious degenerative changes.

Towards the cortical interstitium adhesions were separated by an almost continuous sheet of flat processes of cortical fibroblasts (Figs. 7–9). Since parietal cells have moved away from this interface but adhere to the flanks of the adhesion, a voluminous space between the tuft remnants inside the adhesion and the cortical fibroblasts has come into existence, which may be regarded as tremendously expanded "intra-basement-membrane space" of the basement membrane of the parietal epithelium. The parietal basement membrane is normally multilayered, consisting of several dense layers separated by translucent spaces [28]. Along with the growth of the adhesion, first the translucent spaces expand, followed by the partial or total disintegration of the dense layer material; the outermost dense layer is generally maintained underlying the sheet of fibroblast processes. This expanded space is filled with some kind of a proteinaceous fluid/substance which surrounds the sclerotic formations. Separation of this space from Bowman's space is effected by parietal cells fixing to the flanks of the adhesion. To understand the multiform appearance of those large adhesions it is necessary to imagine that the flanks of an adhesion may not be smooth but may have invaginations (varying in width and depth) into the adherent tuft area.

In one animal in the 28 day group a different type of tuft adhesion was encountered. These were relatively small but – as verified in serial sections – associated with a large cell-rich crescent-like structure overarching the adhesion on all sides (Fig. 9b). The cells were located exclusively within the expanded space of the parietal basement membrane and were clearly parietal cells. Toward the cortical interstitium this structure was demarcated by a layer of cortical fibroblasts.

Mesangial changes

Early stages of the disease were characterized by widespread mesangiolysis attributable to mesangial cell death. At day 3, in parallel with mesangiolytic areas, and more frequently at later stages of the disease, newly produced mesangial tissue was seen, consisting of highly branched mesangial cells embedded in a dense extracel-

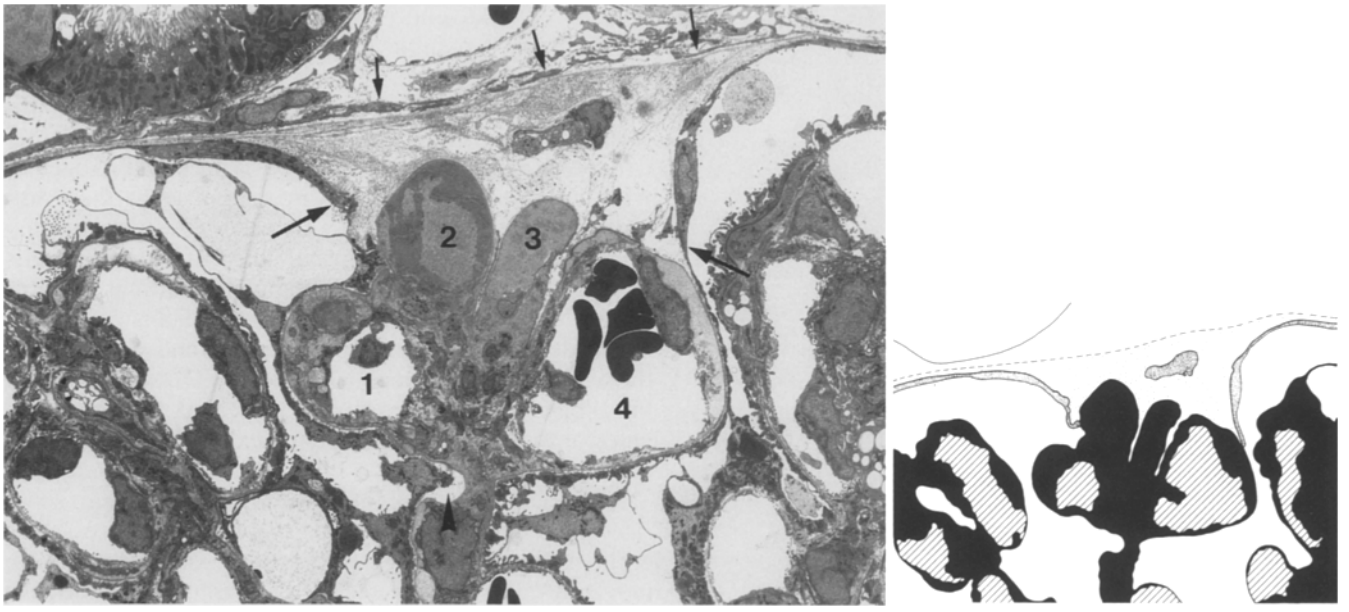

Fig. 7 Intermediate-sized tuft adhesion to Bowman's capsule. The adhesion comprises four capillary loops; two of them (*2*, *3*) are totally hyalinized, while the other two (*1*, *4*) are still patent but accumulations of hyaline material in subendothelial spaces are seen. The parietal epithelium attaches to the flanks of the adhesion (*arrows*). Between the two attachment points the denuded capillary loops are in direct contact with the expanded basement membrane of Bowman's capsule. Towards the cortical interstitium these expanded intra-basement-membrane spaces are delineated by the outermost dense layer of the former multilayered parietal basement membrane followed by a layer of sheet-like processes of cortical fibroblasts (*small arrows*). Note the deteriorated structure of podocytes at the flanks of the adhesion including local detachments from the GBM (*arrowhead*). In the drawing the GBM, including all structures adhering to it from inside, is shown in *black*, patent capillary lumina are *hatched*, parietal cells are *densely stippled* and the expanded intra-basement-membrane space of the parietal basement membrane is *loosely stippled* delineated towards the cortical interstitium by the outermost dense layer (*hatched*) of the former basement membrane. For clarity podocytes are not depicted. MaNe day 28, TEM, ×~1650

lular matrix. The processes of these cells – densely filled with microfilament bundles – extended towards the basement membrane. These areas of solidified mesangial expansion did not show any tendency for further proliferation, but were commonly encountered with a comparable appearance in all stages of the disease (Fig. 10).

Immunocytochemistry

A change in intermediate filament type expression toward desmin has repeatedly been shown to indicate early damage to podocytes [11, 50]. In controls, podocytes contained hardly any desmin (Fig. 11a). By day 1 after serum administration, but most prominently at day 3 (Fig. 11b), a dramatic increase in podocyte desmin expression was seen; thereafter the intensity of desmin staining decreased (Fig. 11c, d).

Discussion

Masugi nephritis is a suitable model for the study of different stages of experimental glomerulonephritis, including progression to glomerulosclerosis [9]. The experimental protocol followed in the present study results in a rapidly progressive disease and a high percentage of segmental glomerulosclerosis only four weeks after initiation of the injury. Damage was seen in all three cell types – endothelial and mesangial cells as well as podocytes – and in addition, in tuft architecture, most probably resulting from the sum of impairments to individual components.

Endothelial lesions developed immediately after initiation of the injury and were extensive. By day 3 recovery was extensive, and by day 7 the endothelium had universally recovered. As noted previously [23], compared with the ubiquity of endothelial damage, thrombosis of capillaries was sparse and – again in agreement with previous studies [42] – most thrombi were cleared during early stages of the disease. However, focally, residuals persisted. Subendothelial spaces remained expanded, becoming filled with proliferating mesangial tissue [23], and some obstruction of capillaries by microthrombi remained. Such occluded capillaries persisted in later stages of sclerosis development, frequently being found incorporated into tuft adhesions to Bowman's capsule (see below).

At the same time as the endothelial damage, widespread mesangiolysis had developed as a result of mesangial cell death. Necrotic mesangial cells and mesangial cell debris were commonly encountered in most early stages of the disease, as was corroborated by a widespread disappearance of mesangial actin staining [44]. As a consequence, failure of mesangial support function led to architectural changes including expansion of mesangial areas, unfolding of capillary patterns and – in conjunction with the loss of podocyte support function (see below) – capillary ballooning. The tuft as a whole,

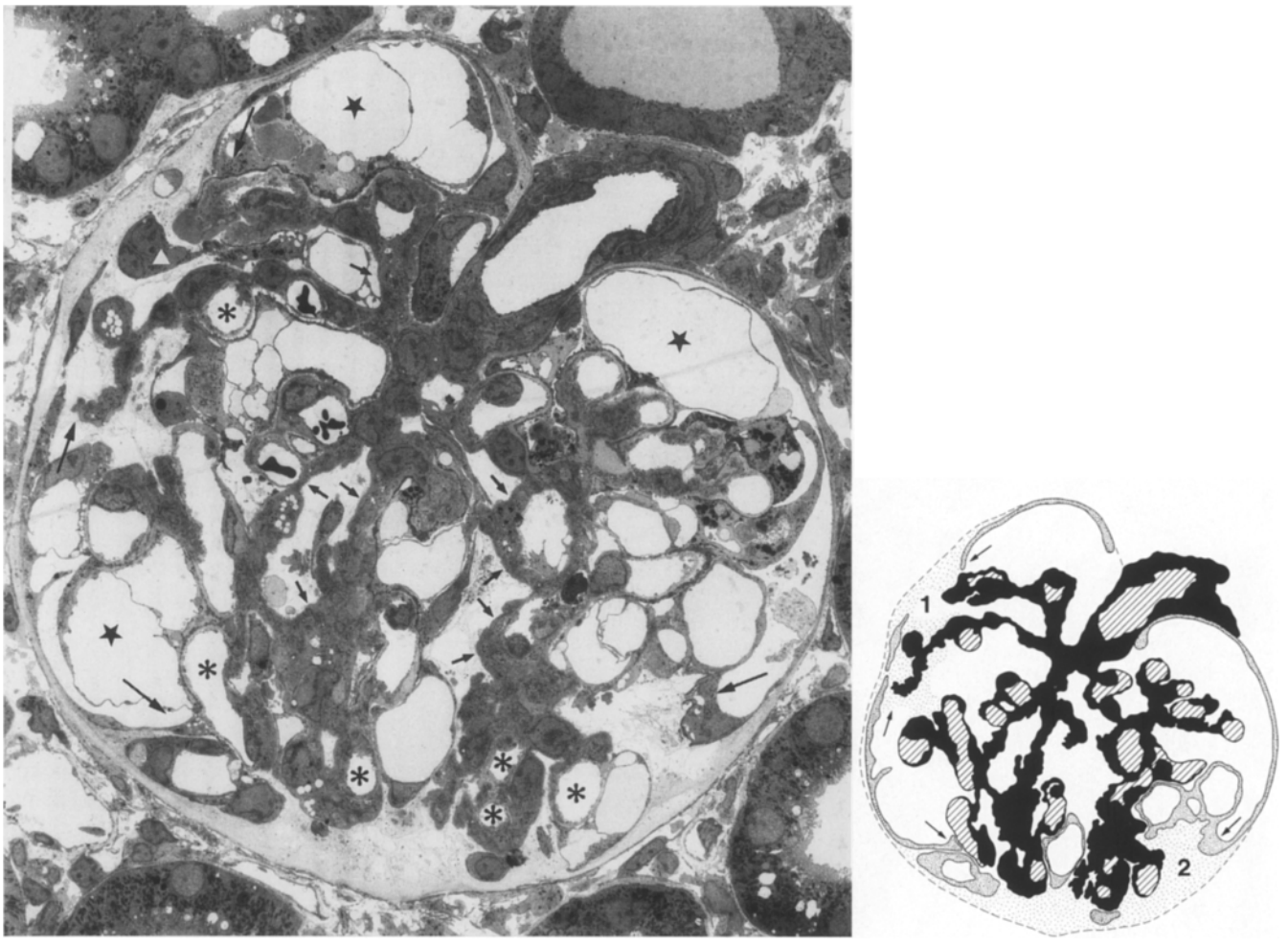

Fig. 8 Glomerular profile with two advanced adhesions. The borders of both adhesions (*1*, *2* in the drawing) are marked by *long arrows*; at these sites the parietal epithelium attaches to the flanks of the adhesion. Between these two points in both adhesions, collapsed, hyalinized or otherwise obstructed capillary loops together with the corresponding mesangial areas (some also collapsed or hyalinized) are surrounded by the expanded intra-basement-membrane space of the parietal basement membrane (*loosely stippled* in the *drawing*). Few capillaries are still patent within the adhesions (*asterisks*). Toward the cortical interstitium the adhesions are delineated by the outermost dense layer of the former multilayered parietal basement membrane, followed by an almost continuous layer of thin sheet-like cortical fibroblast processes. Podocytes have largely disappeared from inside an adhesion (an exception appears to be a binucleated podocyte, marked by a *triangle*). Note widespread podocyte lesions also outside the adhesions including pseudocyst formation (*stars*), accumulation of reabsorption droplets and extensive detachments from the GBM (*small arrows*). In the drawing, the GBM, including all structures that adhere to it from inside, is shown in *black*. Inside this area patent capillaries are *hatched*. Podocytes are not drawn. The parietal epithelium is *densely stippled*. The expanded spaces of the parietal basement membrane are *loosely stippled*; the delineation of these spaces towards cortical fibroblasts is indicated by a *hatched line*. MaNe day 28, TEM, ×~900

an entire lobule, or individual capillaries came much closer to the parietal epithelium than usual; podocyte cell bodies prolapsed into the proximal tubule orifice. The widespread occurrence of those phenomena is also reflected by the significant increase in the ratio of tuft volume to entire corpuscle volume (Table 1). This overall centrifugal expansion of the tuft appears to be rooted in the impairment of the centripetal fixation of glomerular capillaries to the mesangium.

Repair of mesangial lesions started at day 3 and appeared to be generally accomplished by day 7 or 10, when mesangiolytic spaces were replaced by cells and dense matrix. The newly formed mesangial cells were heavily branched, with processes densely stuffed with microfilaments. These processes appeared to have regained mechanical attachment to the GBM, alone or by means of interposed material. Thus, the initial mesangial failure with disconnection of the GBM from its centripetal fixation to mesangial cells and matrix was overcome by mesangial proliferation and matrix deposition, and the slim mesangial axes common to a virgin mesangium were replaced at many sites by clumsy mesangial centres. On comparison of glomeruli from day 10 and day 28 of disease, those expanded mesangial areas appeared unchanged; they did not show any tendency to proliferate further.

It has been almost accepted as a dogma for more than a decade that exuberant mesangial proliferation and matrix synthesis are of dominant pathogenetic relevance to the development of segmental sclerosis. As seen in this and other models of experimental glomerulonephritis [19, 21, 30, 41] mesangial proliferation is not directly involved in this process. Mesangial proliferation occurred in early stages of the disease but did not continue. This is in agreement with previous work [8, 9] showing that in advanced stages of experimental nephritis cell proliferation and matrix synthesis had returned to baseline. Moreover, recent work in Thy-1-mediated glomerular nephritis has disclosed a strong potential of mesangial cells to remodel any overshoot in proliferation [1, 40].

In our view, these areas of solidified mesangial expansion represent some kind of repair, which is successful in the sense that the support function of the mesangium has been reestablished with reconnection of the GBM to the mesangium. There is no question that this repair is no "restitutio ad integrum". It may readily be suggested that such ill-proportioned mesangial centres provide less than perfect support and is more vulnerable to future challenges than the original state. However, it is very clear from the morphology that these newly formed mesangial centres are stable. Sclerosis development from proliferation of such compact mesangial tissue has not been encountered in this or any previous study in which this question has been specifically addressed [21, 30, 41].

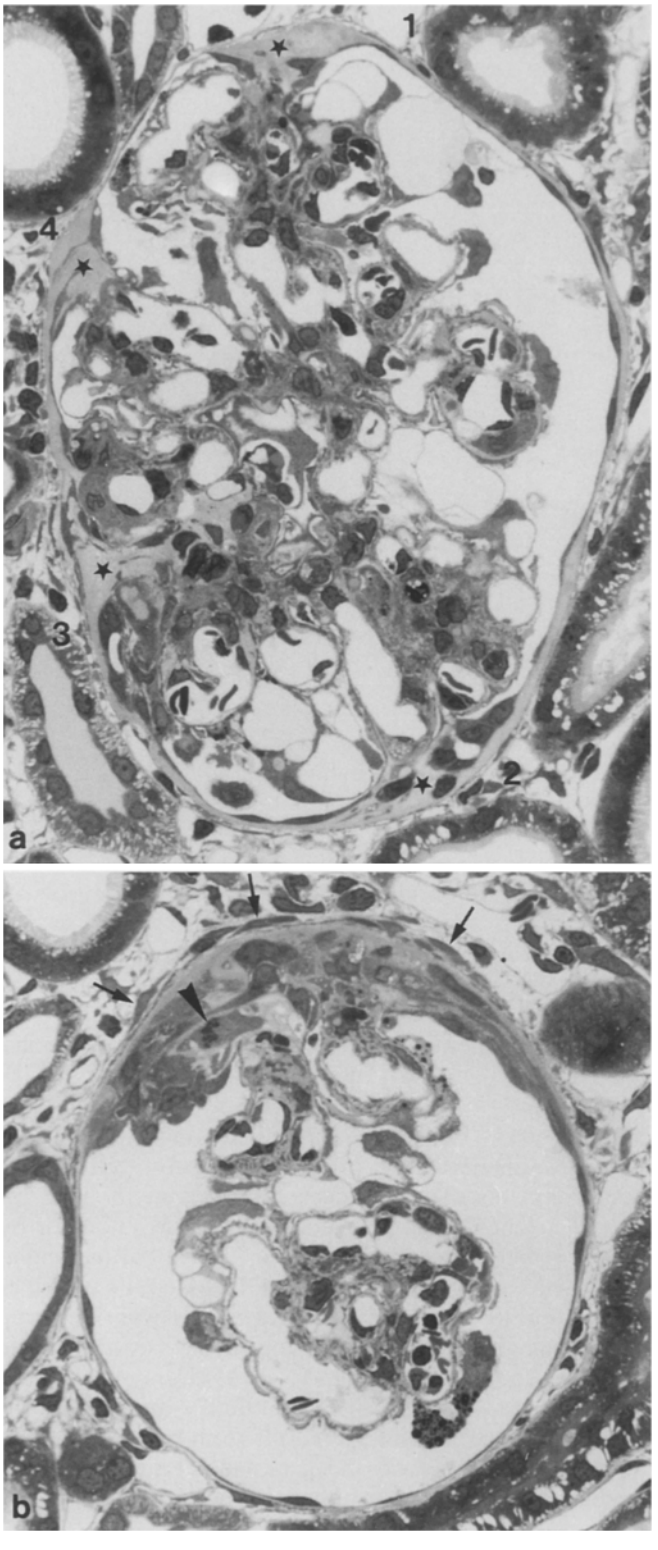

Podocyte injury

Four hours after serum administration podocytes looked fairly normal, but after 1 day dramatic and extensive changes in podocyte structure were seen – again in agreement with previous studies [17, 23]. The most prominent was foot process effacement, which was encountered in almost every podocyte. In a separate paper [44] we have shown that within the "fused" podocyte portions the microfilament system of podocyte foot processes had developed into a prominent cytoskeletal mat associated with the basal cell membrane. Whether the concomitant expression of the intermediate filament protein desmin (which is generally taken as to indicate early podocyte injury [11, 50]) is an immanent part of an overall cytoskeletal rearrangement is unknown.

Functionally, the conspicuous changes in the microfilament system have been interpreted as a reinforcement of the contractile apparatus of podocytes, to counteract increased distending forces. An increase in mechanical challenge to podocytes may originate from several fac-

Fig. 9a, b Tuft adhesions to Bowman's capsule/segmental sclerosis. **a** Glomerular profile with multiple tuft adhesions (*1–4*); the largest one (*3*) clearly represents what is generally regarded as segmental sclerosis. All four adhesions exhibit the same pattern: parietal cells attached to the flanks delineate funnel-shaped spaces (*stars*) containing the adherent tuft structures and separated from the cortical interstitium by processes of cortical fibroblasts. **b** A comparatively small adhesion is associated with a large cellular crescent overroofing the adhesion towards all sides (verified in the corresponding section series). The cells of this crescent appear to be parietal cells located in the expanded parietal intra-basement-membrane space, clearly delineated toward the cortical interstitium by cortical fibroblasts (*arrows*). A mitosis is seen within the crescent (*arrowhead*). MaNe day 28, LM, **a** ×~440; **b** ×~460

tors. First, as shown by two groups [2, 26] glomerular capillary pressures are elevated in Masugi nephritis and may be amplified in their "destructive effectiveness" in ballooned capillaries according to Laplace's law [6]. Moreover, impairment of the substructure of the GBM due to the antibody attack [48] may result in decreased tensile strength of the GBM, augmenting the burden of podocytes to counteract capillary wall expansion. Compared with the ubiquity of foot process effacement, all other early changes in podocyte structure were less prominent.

In the later stages of the disease, in contrast to the fairly uniform reparative changes of the endothelium and mesangium, the development of podocyte lesions was complex. On the one hand, reparative processes were obvious, on the other progressive podocyte damage was encountered in a major proportion of glomeruli. By day 28 reorganization of a foot process pattern could be clearly seen. The fractional area of the outer capillary surface covered by fused podocyte portions (thus lacking an interdigitating foot process pattern) had decreased from about 90% at day 10 to about 50%. Reestablishment of a foot process pattern was mostly seen in tuft areas where capillary and mesangial lesions had obviously been restored earlier in the course of the disease (see [44]).

However, in other glomeruli, in other lobules of glomeruli in the neighbourhood of recovering areas, progressive structural degeneration was seen. Those deteriorating areas were consistently associated with severe podocyte injury, including detachments and tuft adhesions to Bowman's capsule. Like the development of sclerosis in other models [19, 21, 30] and as in previous work in Masugi nephritis [17], it is evident that FSGS develops on the basis of podocyte detachment from the GBM.

Development of segmental sclerosis

All stages of sclerosis development were seen in kidneys from day 10 and day 28 after serum administration. As is characteristic for the focal development of the disease, early and late stages may be encountered side by side in a single section. Our synthesis of a sequence of serial steps in the development of segmental glomerulosclerosis answers the question as to what would be the most plausible sequelae of the many different lesions found in these kidneys. The main aspects of this sequence are summarized in the schematic drawing seen in Fig. 12.

Two lesions appear to be of pivotal importance for the development of segmental sclerosis. The first is severe podocyte injury including detachments from peripheral capillary loops. The second is expansion of the tuft, leading locally or globally to a close approximation of the tuft to Bowman's capsule, seen most spectacularly in prolapse of tuft structures into the tubular orifice (possibly progressing to a tip lesion; [15]). In Masugi nephritis those expansile tuft movements may be encountered at any site on the tuft circumference. They represent architectural lesions, resulting from the loss of support function. In Masugi nephritis both supporting systems [22, 29] (mesangium and podocytes) are severely impaired, leading to the entire spectrum of architectural lesions [20] including mesangial expansion, unfolding of capillary patterns and capillary ballooning. As a consequence,capillary loops bulge toward Bowman's capsule,increasing the chance of apposition of a naked capillary loop to the parietal epithelium (Fig. 12a, b).

Direct contact of a "naked" portion of the GBM and the parietal epithelium allows the parietal cells to attach to the GBM (Fig. 12c). At these sites, parietal cells lose their lateral contact with neighbouring parietal cells and establish firm contact with the GBM. Frequently, two neighbouring parietal cells attach to the same capillary loop, leaving a gap between the two attachement sites, where GBM and the parietal basement membranes attach directly to each other. A gap in the parietal epithelium has thus come into existence, resulting in direct contact of the GBM and the parietal basement membrane. This gap may represent a filtration route from a glomerular capillary into the cortical interstitium.

The growth of a "one-loop adhesion" occurs by spreading to adjacent capillary loops (Fig. 12d). The mechanism is more or less the same as in establishment of the first contact. In the vicinity, especially at the flanks of an adhesion, podocytes continue to degenerate and to detach from capillary loops (see below). The parietal epithelium encroaches on the tuft by moving along the denuded GBM to neighbouring capillaries. The contact with the first capillaries is lost, so that they are pushed into the centre of the growing adhesion. As a consequence the adhesion achieves a broad area of contact with the periglomerular interstitium.

Inside a progressing adhesion, capillaries either collapse or become occluded by hyaline material or by microthrombosis. Hyalinosis is believed to develop from bulk filtration through capillary walls denuded of podocytes [35, 38]. High-molecular-weight proteins (globulins) cannot pass through the GBM and accumulate behind the GBM leading to hyalinosis. Thus, the formation of hyalinosis depends on some continuing filtration. If filtration ceases locally for some reason (thrombosis in an upstream capillary), the corresponding capillaries simply collapse resulting in the formation of wrinkled GBM profiles. Obstruction of capillaries by microthrombosis appears to occur in varying frequencies along with the growth of an adhesion. Microthrombosis also occurs in most early stages of the disease and may well represent a relevant factor contributing to the detachment of a podocyte from a capillary and, consequently, to the formation of a tuft adhesion [25, 34]. Microthrombosis may be an antecedent of adhesion formation rather than its consequence.

Podocytes disappear from inside an adhesion simply by cellular dissolution. If, as rarely happens, a podocyte is encountered inside an adhesion, it exhibits severe lesions and its extinction appears to be imminent. Inside the GBM, some cells have survived, apparently squeezed

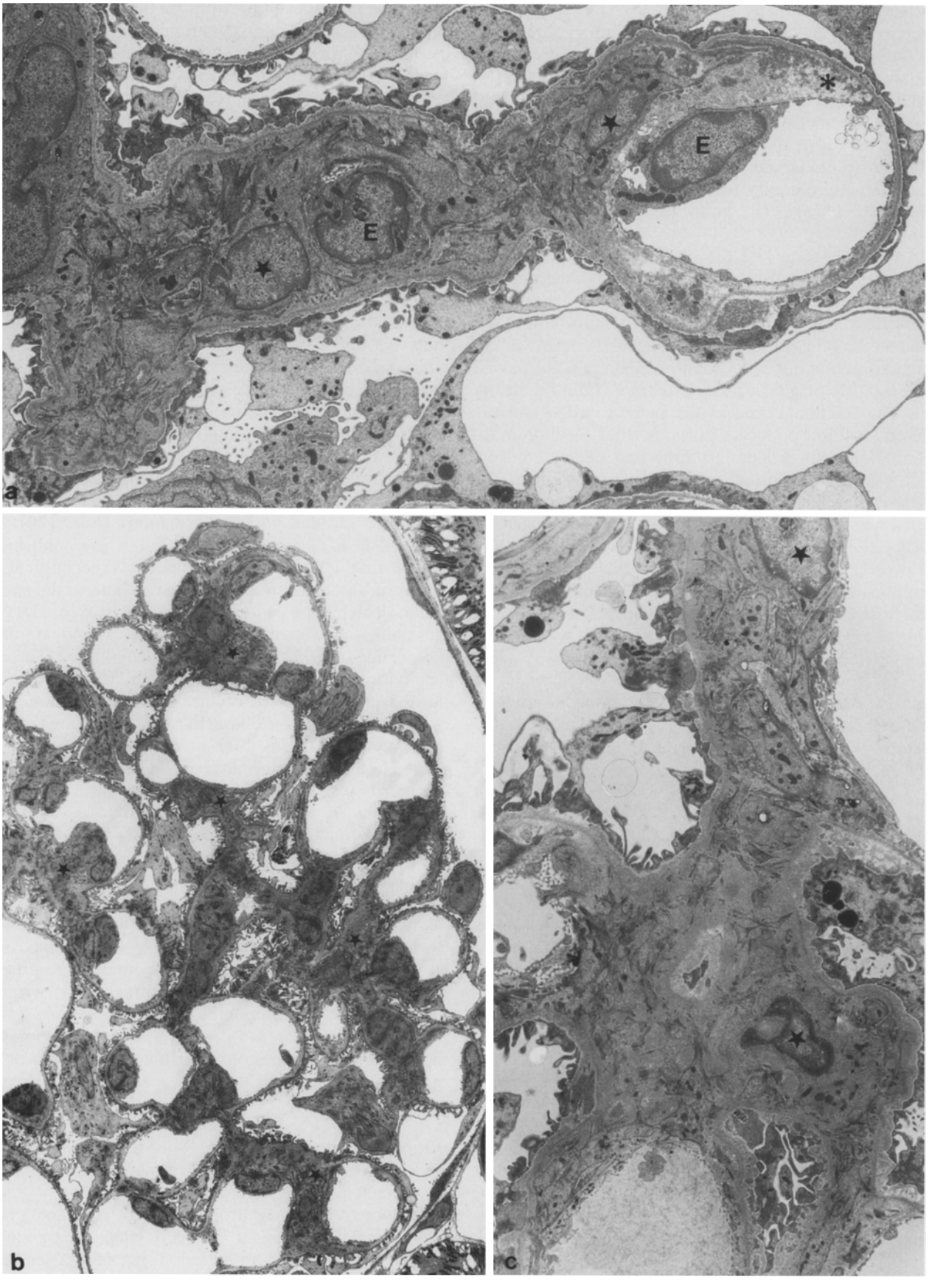
E
E
a
b
c

between collapsed GBM profiles. No attempts have been made to distinguish whether these are former mesangial or endothelial cells. Signs of proliferation have never been encountered; in fact, resident cells obviously decrease in number along with the growth of the adhesion, in agreement with the observation of considerable apoptosis in areas inside the GBM in the 5/6 nephrectomy model of sclerosis development [45]. However, macrophages densely filled with lysosomal elements are frequently encountered, either as individual cells or assembled as clusters, suggesting local proliferation [24]. Macrophages are most regularly seen in conjunction with the obstruction of capillaries by microthrombi.

The most typical structures of an advanced adhesion are "sclerotic formations", collapsed, hyalinized or otherwise occluded capillaries and former mesangial areas. These structures are all bounded by the (former) GBM, which also constitutes their major component. They are enclosed in a prominent fluid-rich space, which represents an expansion of the parietal basement membrane of Bowman's capsule. It appears that filtration across the denuded GBM accounts for the development of this space. By the attachment of a podocyte-deprived glomerular capillary to the parietal basement membrane filtration into the periglomerular interstitium may occur. The parietal basement membrane itself, which is a multilayered structure [28], may be regarded as the first interstitial component. This basement membrane expands into a voluminous space, spreading like a growing cap over an entire hemisphere of the glomerulus. It appears reasonable to suggest that the high-pressure gradient between a glomerular capillary and the interstitium leads to fluid filtration resulting in the expansion of the intra-basement-membrane space and its filling with a proteinaceous fluid.

Towards the cortical interstitium the space is delineated by the outermost dense layer of the former multilayered basement membrane, followed by a continuous cover of sheet-like processes of peritubular fibroblasts. This fibroblast layer has obviously been established in direct response to the changes in Bowman's capsule. Moreover, it is attractive to argue that the proliferative response of the peritubular interstitium frequently seen in areas of fo-

◀ **Fig. 10a–c** Mesangial proliferation. **a** Mesangial axes (day 10) containing several mesangial cells (nuclei are marked by *stars*) with many processes stuffed with microfilament bundles and extending toward the GBM. Apart from subendothelial accumulations (*asterisk*) comparatively little extracellular material is seen within the mesangial space. Podocytes show foot process effacement and are partly disconnected from the GBM. The gaps beneath the disconnections are filled by dark staining material (*E* endothelial cell). **b** Overview of a glomerular lobule (day 28) showing widespread solidified mesangial expansion (*stars*) in an area of almost complete recovery of an interdigitating podocyte foot process pattern. **c** Mesangial axes (day 28) with highly branched mesangial cells (only two nuclei are hit, marked by *stars*). The mesangial processes contain microfilament bundles and extend toward the basement membrane. They are embedded into a dark-staining extracellular matrix. Note that this expanded but solidified mesangial tissue from day 10 (**a**) and day 28 (**c**) is fairly identical in elaboration. **a** MaNe day 10, TEM, ×~4300; **b** MaNe day 28, TEM, ×~3000; **c** MaNe day 28, TEM, ×~3600

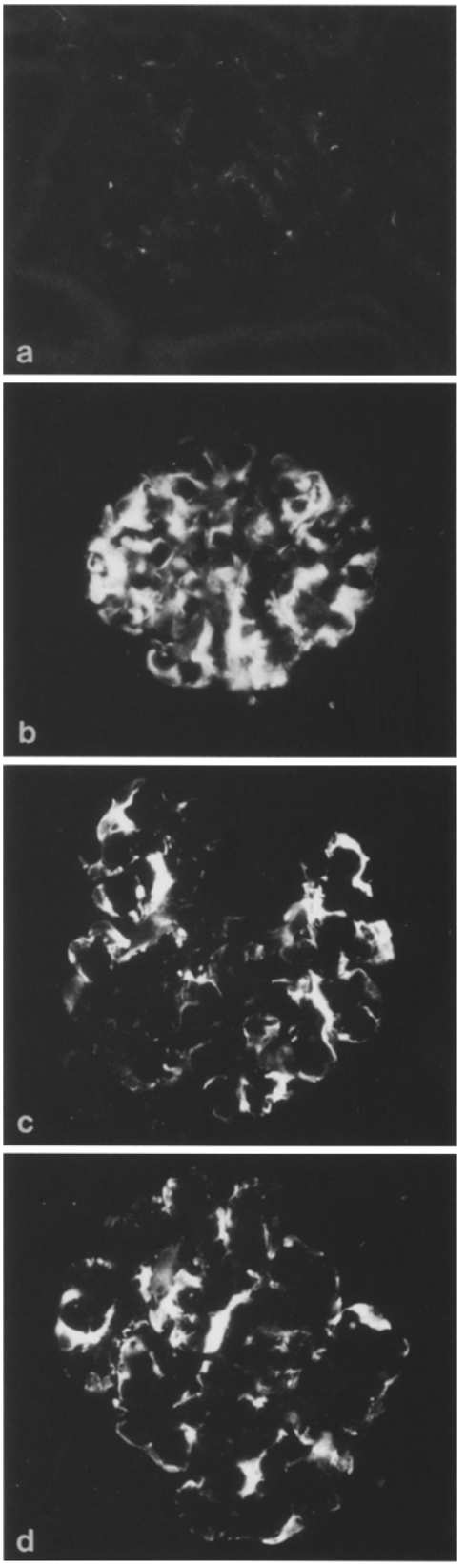

Fig. 11a–d Desmin expression in podocytes. **a** Podocytes in controls do not express desmin in substantial amounts. **b** The situation changes dramatically during the early development of the disease. Desmin expression in podocytes is most prominent at day 3 and stays prominent in later stages of the disease at **c** day 10 and **d** day 28. MaNe, FITC-conjugated immunocytochemistry with an antibody against desmin, LM, ×~350

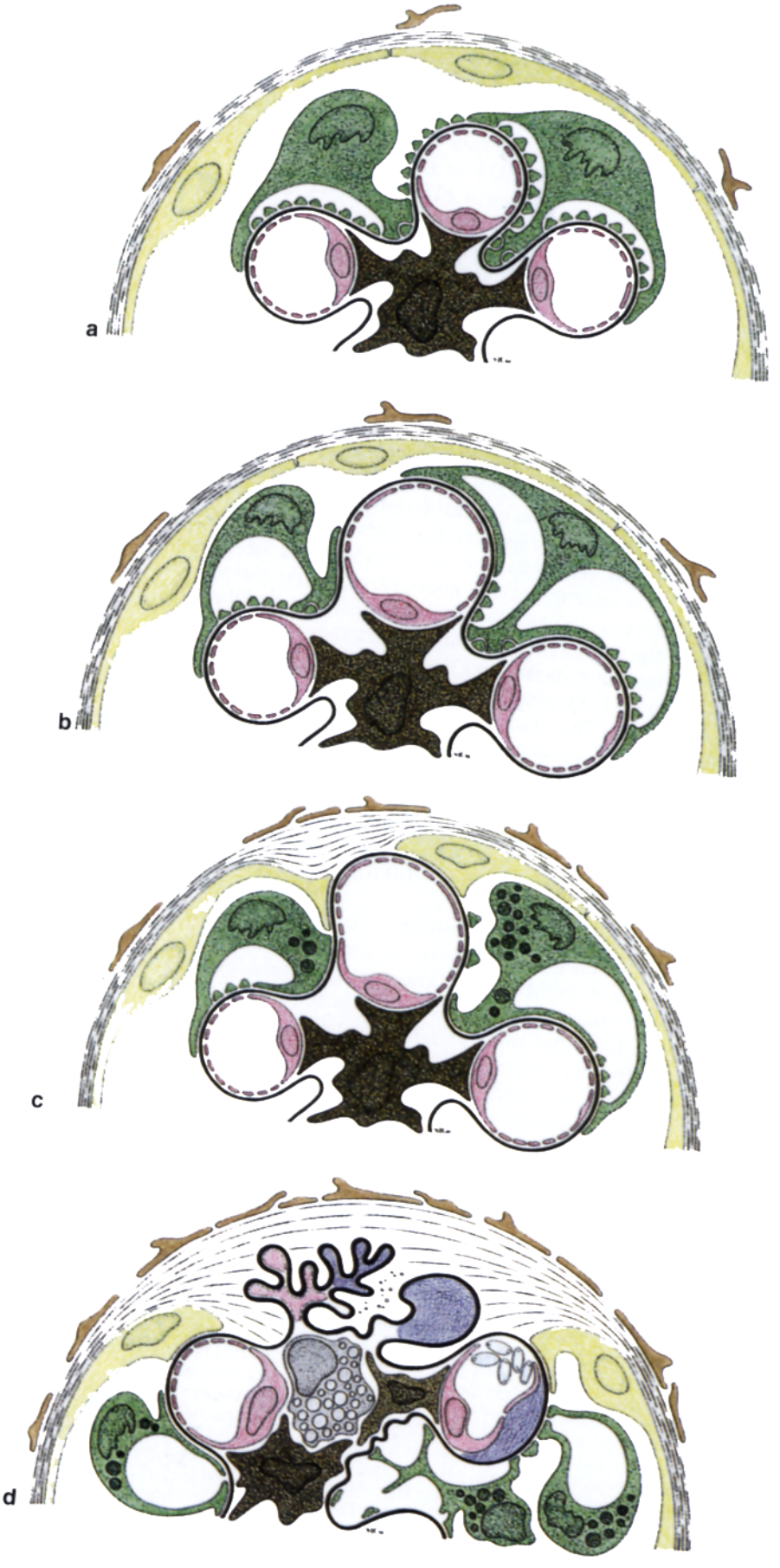

Fig. 12a–d Schematics to show the development of a tuft adhesion to Bowman's capsule. The parietal epithelium is shown in *yellow*, podocytes in *green*, endothelial cells in *red*, mesangial cells in *light brown*, and the GBM in *black*; the parietal basement membrane is *hatched*, indicating its multilayered structure. **a** Normal situation. Peripheral capillary loops and the parietal epithelium are separated from each other by Bowman's space. **b** Apposition. A dilated and partly denuded capillary loop bulges toward Bowman's capsule and becomes apposed to the parietal epithelium. **c** Adhesion. Parietal cells dissolve from each other and attach to the flanks of the "naked" capillary loop. A gap in the parietal epithelium comes into existence, where the GBM adheres directly to the parietal basement membrane; the parietal basement expands in itself. **d** Growth of the adhesion. Podocytes at the flanks of the adhesion undergo degenerative changes and finally die. The adhesion grows by encroaching parietal cells along the denuded GBM to neighbouring capillaries. The adherent area enlarges, and the parietal basement membrane expands, becoming a voluminous space that is separated from the cortical interstitium by a layer of sheet-like processes of cortical fibroblasts. Inside the adhesion a plethora of lesions are seen. Podocytes have disappeared. Capillaries are collapsed or obstructed by hyalinosis (shown in *violet*) or by microthrombosis. Macrophages (shown in *grey*) invade into capillaries and mesangial areas

cal glomerulosclerosis is another consequence of continuing fluid filtration into the periglomerular interstitium.

In summary, beginning with a firm attachment of a capillary to Bowman's capsule, a process is started that will terminate in segmental sclerosis. Segmental sclerosis in this model consists of an adherent tuft area with collapsed or obstructed capillaries, disappearance of cellular elements, and accumulation of hyaline material, but little if any scar collagen. The subsequent fate of a glomerulus with segmental sclerosis is the encroachment of the sclerotic process onto the entire tuft followed by the final collapse of the structure and secondary organization with deposition of fibrous tissue. This process has not been investigated in this study; comparatively few glomeruli had progressed to such terminal stages.

What underlies progressive podocyte degeneration?

The regenerative potential of mesangial and endothelial cells largely depends on cell proliferation. Podocytes do not have the capability for cell replication [13, 30, 31]. They are capable of nuclear but not of cell body division; in response to massive mitogenic stimulation, podocytes may enter the cell division cycle but do not complete it resulting in bi(multi)nucleated cells [21]. In the present study mitotic figures in podocytes and many binucleated podocytes were found without any increase in podocyte cell number, in agreement with previous findings. The inability of podocytes to multiply is a fundamental property of these cells, which has two important consequences. First, the only, limited way for podocytes to cope with increasing challenges is by hypertrophy (binucleated cells are hypertrophied cells), and second, "outmatched" podocytes cannot be replaced.

Detachment of a podocyte from the basement membrane indicates the failure of this podocyte to cover the outer surface of a glomerular capillary. Let us imagine for a moment that podocytes do have an ability to replicate; denuded GBM areas would possibly be transient, like endothelial detachments. Since podocytes cannot proliferate, the only way to repair such defects is by cell hypertrophy of neighbouring podocytes, with the development of additional or larger processes. It appears that the hypertrophic potential of podocytes is limited, especially in situations where they are already injured by preceding challenges.

This scenario helps us to understand why severe damage to a podocyte or a group of podocytes has a good chance of leading to tuft adhesion. This scenario does not explain why, when an adhesion is established but the damaging mechanism is no longer in action, podocytes associated with an adhesion continue to degenerate. Two mechanisms may be suggested to contribute to their vulnerability in this situation. Podocytes situated at the flanks of an adhesion, may be exposed to unbalanced mechanical stress [30]. Podocytes at this site are partly fixed to the adherent tuft area and partly to the unaffected, possibly still movable, tuft area. In normal conditions, podocytes may be expected to float in the filtrate of Bowman's capsule, but those at the flanks of or inside an adhesion may be able to float with some of their cell portions, with others not. In a theoretical analysis [4] mechanical deformations of podocyte surfaces at their attachment site were shown to have the strongest effect in lifting the cells from the GBM. Second, podocytes at the flanks of an adhesion are frequently densely filled with absorption droplets, probably resulting from massive protein leakage at these sites. It appears that lysosomal degradation in those podocytes cannot cope with the amount of engulfed material eventually terminating in vacuolar degeneration. The appearance of podocytes overloaded with absorption droplets and other lysosomal elements would be consistent with a mechanism by which overchallenge of the lysosomal system leads to self-digestion, resulting in cell dissolution.

Location of tuft adhesions

Tuft adhesions were encountered at any point of the tuft circumference. This distribution pattern has previously been suggested as characteristic of random damage to the glomerulus [14]. The crucial lesions initiating sclerosis development in the present model are severe deterioration in tuft architecture leading to a local bulging of capillaries towards Bowman's capsule and denudation of those capillaries. The first event, the architectural lesion, depends on both mesangial and podocyte failure, the second, the denudation, on podocyte degeneration. It appears that the concurrence of both events is random with respect to a particular glomerulus, accounting for the focal distribution of the injury, and also with respect to the locus within the tuft, accounting for the variable segmental distribution. This pattern must be seen in contrast to a preferential development of segmental sclerosis at the vascular pole. This second pattern is characteristic for models in which high glomerular pressures are thought to lead directly to overchallenge and subsequent damage to podocytes, especially those that service the primary branches of the afferent arteriole [6].

Repair versus progression to sclerosis

Repair processes leading to the reconstitution of "filtering" capillaries and progression of lesions to segmental glomerulosclerosis are seen side by side in the same kidney, and even in the same glomerulus. At first glance, it appears contradictory that reparative and destructive mechanisms are in action simultaneously.

Sclerosis development is an irreversible process. As soon as a certain stage of sclerosis development is reached (we would suppose that the formation of a tuft adhesion represents this stage), this process will inevitably proceed to the degeneration of the glomerulus. However, this process does not directly affect the repair processes of presclerotic lesions in neighbouring glomeruli

nor – at least in the beginning – in neighbouring lobules of the same glomerulus. The progressive character of FSGS is thought to be based on the increasing overload of the remaining glomeruli leading to the initiation of sclerotic lesions in this or that particular glomerulus [3, 12]. In the present model the incidence of sclerosis amounts to 23% (Table 1) and thus has become the dominant process; therefore repair processes in other glomeruli must be considered of limited relevance.

Conclusion

Focal segmental glomerulosclerosis represents a stereotyped degeneration pattern of a glomerulus common to a great variety of glomerular diseases. Most notably, this pattern underlies the progressive nephron loss and thus, progressive loss of renal function in end-stage renal disease. The sequence of structural changes seen in Masugi nephritis in this and an older study [17] has been recognized in various other rat models, including DOCA-salt hypertension [19], and the development of glomerulosclerosis subsequent to UNX in young animals [30] and after long-term treatment with FGF-2 [21], in the Milan normotensive rat [7] and in the fawn-hooded rat (unpublished).

Thus, the development of focal segmental glomerulosclerosis apparently follows a uniform pathway that is independent of the initial damaging mechanism. We propose that the monotonous character of this process is rooted in the inability to replace deceased podocytes. Podocytes are unable to replicate; thus the only way to compensate the function of a worn out podocyte is by hypertrophy of any remaining cells. Beyond certain limits, hypertrophy of podocytes increases their vulnerability to any further challenge, starting up a vicious circle. This accounts for the uniformity of glomerular degeneration and for the progressive character of chronic renal failure.

Acknowledgements This study was supported by the Deutsche Forschungsgemeinschaft, project Kr 546/9–1. We thank R. Nonnenmacher for the art work, I. Ertel for photographic work and M. Schuchardt for secretarial assistance.

References

1. Baker AJ, Mooney A, Hughes J, Lombardi D, Johnson RJ, Savill J (1994) Mesangial cell apoptosis: The major mechanism for resolution of glomerular hypercellularity in experimental mesangial proliferative glomerulonephritis. J Clin Invest 94:2105–2116
2. Blantz RC, Wilson B (1976) Acute effect of antiglomerular basement membrane antibody on the process of glomerular filtration in the rat. J Clin Invest 58:899–911
3. Brenner BM, Meyer TW, Hostetter TH (1982) Dietary protein intake and the progressive nature of kidney disease: the role of hemodynamically mediated glomerular injury in the pathogenesis of progressive glomerular sclerosis in aging, renal ablation, and intrinsic renal disease. N Engl J Med 307:652–659
4. Cho CR, Lumsden CJ, Whiteside CI (1993) Epithelial cell detachment in the nephrotic glomerulus: a receptor co-operativity model. J Theoret Biol 160:407–426
5. Cochrane CG, Unanue ER, Dixon FJ (1965) A role for polymorphonuclear leukocytes and complement in nephrotoxic nephritis. J Exp Med 122:99–116
6. Daniels BS, Hostetter TH (1990) Adverse effects of growth in the glomerular microcirculation. Am J Physiol 258: F1409–F1416
7. Deppe M (1983) Altersabhängige morphologische Veränderungen der Glomeruli bei Mailänder Ratten. Thesis, University of Hannover
8. Downer G, Phan SH, Wiggins RC (1988) Analysis of renal fibrosis in a rabbit model of crescentic nephritis. J Clin Invest 82:998–1006
9. El Nahas AM (1993) Masugi nephritis: a model for all seasons. In: Gretz N, Strauch M (eds) Experimental and genetic rat models of chronic renal failure. Karger, Basel, pp 49–67
10. El Nahas AM, Lechler R, Zoob SN, Res AJ (1985) Progression to renal failure after nephrotoxic nephritis in rats studied by renal transplantation. Clin Sci 68:15–21
11. Floege J, Alpers CE, Sage EH, Pritzl P, Gordon K, Johnson RJ, Couser WG (1992) Markers of complement dependent and complement independent glomerular visceral epithelial cell injury in vivo. Lab Invest 67:486–497
12. Fogo A, Ichikawa I (1992) Glomerular growth promotor – the common channel to glomerular sclerosis. In: Mitch WE, Stein JH (eds) The progressive nature of renal disease. (Contemporary issues in nephrology, vol 26) Churchill Livingstone, New York, pp 23–54
13. Fries JW, Sandstrom DJ, Meyer TW, Rennke HG (1989) Glomerular hypertrophy and epithelial cell injury modulate progressive glomerulosclerosis in the rat. Lab Invest 60: 205–218
14. Howie AJ, Kizaki T, Beaman M, Morland CM, Birtwistle RJ, Adu D, Michael J, Williams AJ, Walls J, Matsuyama M, Shimizu F (1989) Different types of segmental sclerosing glomerular lesions in six experimental models of proteinuria. J Pathol (Lond) 157:141–151
15. Howie AJ, Lee SI, Sparke J (1995) Pathogenesis of segmental glomerular changes at the tubular origin, as in the glomerular tip lesion. J Pathol (Lond) 177:191–199
16. Kaissling B, Kriz W (1982) Variability of intercellular spaces between macula densa cells: a transmission electron microscopic study in rabbits and rats. Kidney Int 22[Suppl 12]:S-9–S-17
17. Kondo Y, Akikusa B (1982) Chronic Masugi nephritis in the rat. An electron microscopic study on evolution and consequences of glomerular capsular adhesions. Acta Pathol Jpn 32: 231–242
18. Koshino Y, Cashman SJ, Ryan J (1989) Modulation of antibody-mediated glomerular injury in nephrotoxic nephritis by antibodies to tumor necrosis factor. Nephrol Dial Transplant 4:837
19. Kretzler M, Koeppen-Hagemann I, Kriz W (1994) Podocyte damage is a critical step in the development of glomerulosclerosis in the uninephrectomised-desoxycorticosterone rat. Virchows Arch [A] 452:181–193
20. Kriz W, Elger M, Nagata M, Kretzler M, Uiker S, Koeppen-Hagemann I, Tenschert S, Lemley KV (1994) The role of podocytes in the development of glomerular sclerosis. Kidney Int 45[Suppl 45]:S-64–S-72
21. Kriz W, Hähnel B, Rösener S, Elger M (1995) Long-term treatment of rats with FGF-2 results in focal segmental glomerulosclerosis. Kidney Int 48:1435–1450
22. Kriz W, Elger M, Mundel P, Lemley KV (1995) Structure-stabilizing forces in the glomerular tuft. J Am Soc Nephrol 5: 1731–1739
23. Kühn K, Ryan GB, Hein SJ, Galaske RG, Karnovsky MJ (1977) An ultrastructural study of the mechanism of proteinuria in rat nephrotoxic nephritis. Lab Invest 36:375–387
24. Lan HY, Nikolic-Paterson DJ, Mu W, Atkins RC (1995) Local macrophage proliferation in the progression of glomerular and tubulointerstitial injury in rat anti-GBM glomerulonephritis. Kidney Int 48:753–760

25. Lee LK, Meyer TW, Pollock AS, Lovett DH (1995) Endothelial cell injury initiates glomerular sclerosis in the rat remnant kidney. J Clin Invest 96:953–964
26. Maddox DA, Bennet CM, Deen WM, Glassock RJ, Knutson D, Daugharty TM, Brenner BM (1975) Determinants of glomerular filtration in experimental glomerulonephritis in the rat. J Clin Invest 55:305–318
27. Masugi M, Tomizuka Y (1931) Über die spezifischen zytotoxischen Veränderungen der Niere und der Leber durch das spezifische Antiserum (Nephrotoxin und Hepatotoxin). Zugleich ein Beitrag zur Pathogenese der Glomerulonephritis. Trans Jpn Pathol Soc 21:329–341
28. Mbassa G, Elger M, Kriz W (1988) The ultrastructural organization of the basement membrane of Bowman's capsule in the rat renal corpuscle. Cell Tissue Res 253:151–163
29. Mundel P, Kriz W (1995) Structure and function of podocytes: an update. Anat Embryol 192:385–397
30. Nagata M, Kriz W (1992) Glomerular damage after uninephrectomy in young rats. II. Mechanical stress on podocytes as a pathway to sclerosis. Kidney Int 42:148–160
31. Nagata M, Yamaguchi Y, Komatsu Y, Ito K (1995) Mitosis and the presence of binucleate cells among glomerular podocytes in diseased human kidneys. Nephron 70:68–71
32. Neugarten J, Feiner HD, Schacht RG (1982) Aggravation of experimental glomerulonephritis by superimposed clip hypertension. Kidney Int 22:257–263
33. Neugarten J, Kamimetsky B, Feiner HD (1985) Nephrotoxic serum nephritis with hypertension: amelioration by antihypertensive therapy. Kidney Int 28:135–139
34. Noris M, Remuzzi G (1995) New insights into circulation cell-endothelium interactions and their significance for glomerular pathophysiology. Am J Kidney Dis 26:541–548
35. Olson JL, Uradaneta AG, Heptinstall RH (1985) Glomerular hyalinosis and its relation to hyperfiltration. Lab Invest 52:387
36. O'Meara YM, Natori Y, Minto AW, Goldstein DJ, Manning EC, Salant DJ (1992) Nephritogenic antiserum identifies a b1-integrin on rat glomerular epithelial cells. Am J Physiol 262: F1083–F1091
37. Rennke HG (1994) How does glomerular epithelial cell injury contribute to progressive glomerular damage? Kidney Int 45[Suppl 45]:S-58–S-63
38. Rennke HG, Anderson S, Brenner BM (1992) The progression of renal disease: structural and functional correlations. In: Tisher CC, Brenner BM (eds) Renal Pathology. Lippincott, Philadelphia, pp 116–139
39. Sakai T, Kriz W (1987) The structural relationship between mesangial cells and basement membrane of the renal glomerulus. Anat Embryol 176:373–386
40. Savill J, Johnson RJ (1995) Glomerular remodelling after inflammatory injury. Exp Nephrol 3:149–158
41. Schwartz MM, Bidani AK (1991) Mesangial structure and function in the remnant kidney. Kidney Int 40:226-237
42. Shigematsu H (1970) Glomerular events during the initial phase of rat Masugi nephritis. Virchows Archiv [B] 5:187–200
43. Shirato I, Sakai T, Fukui M, Tomino Y, Koide H (1993) Widening of capillary neck and alteration of extracellular matrix ultrastructure in diabetic rat glomerulus as revealed by computer morphometry and improved tissue processing. Virchows Arch 423:121–129
44. Shirato I, Sakai T, Kimura K, Tomino Y, Kriz W (1996) Cytoskeletal changes in podocytes associated with foot process effacement in Masugi nephritis. Am J Pathol 148:1283–1296
45. Sugiyama H, Kashihara N, Makino H, Yamasaki Y, Ota Z (1996) Apoptosis in glomerular sclerosis. Kidney Int 49: 103–111
46. Syndrey M, Naish P (1979) The mediation of the localization of polymorphonuclear leukocytes in glomeruli during the autologous phase of nephrotoxic nephritis. Clin Exp Immunol 35:350–355
47. Tomosugi NI, Cashman SJ, Hay H (1989) Modulation of antibody-mediated glomerular injury in vivo by bacterial polysaccharide, tumor mecrosis factor and IL-1. J Immunol 142: 3083–3090
48. Vogt A, Bockhorn H, Kozima K, Sasaki M (1968) Electron microscopic localization of the nephrotoxic antibody in the glomeruli of rats after intravenous application of purified nephritogenic antibody-ferritin conjugates. J Exp Med 127: 867–878
49. Weibel ER (1979) Stereological methods. Practical methods for biological morphometry. Academic Press, London
50. Yaoita E, Kawasaki K, Yamamoto T, Kihara I (1990) Variable expression of desmin in rat glomerular epithelial cells. Am J Pathol 136:899–908